ISSN 0031-918X, Physics of Metals and Metallography, 2018, Vol. 119, No. 8, pp. 741–746. © Pleiades Publishing, Ltd., 2018.
Original Russian Text © D.A. Perminov, A.P. Druzhkov, V.L. Arbuzov, 2018, published in Fizika Metallov i Metallovedenie, 2018, Vol. 119, No. 8, pp. 787–793.

STRUCTURE, PHASE TRANSFORMATIONS, AND DIFFUSION

Positron Annihilation Spectroscopy of the Accumulation of Vacancy Defects in an Aging Fe–Ni–Al Alloy Irradiated at 573 K

D. A. Perminov[a], *, A. P. Druzhkov[a], and V. L. Arbuzov[a]

[a] *Mikheev Institute of Metal Physics, Ural Branch, Russian Academy of Sciences, Ekaterinburg, 620137 Russia*

**e-mail: perminov@imp.uran.ru*

Received November 8, 2017; in final form, March 13, 2018

Abstract—The influence of intermetallic Ni_3Al precipitates on the accumulation of vacancy defects in aged Fe–Ni–Al alloy at the initial stages of electron irradiation (5×10^{-4} dpa) at a temperature of 573 K has been studied using positron annihilation spectroscopy. The obtained results demonstrate that intermetallic precipitates inhibit the process of the accumulation of vacancy defects under irradiation. It has been found that these precipitates facilitate the mutual recombination of point defects that form under irradiation. This effect has been attributed to elastic stresses at the precipitate–matrix boundaries.

Keywords: iron–nickel alloys, intermetallic precipitates, electron irradiation, radiation defects, defect recombination, positron annihilation

DOI: 10.1134/S0031918X18080094

INTRODUCTION

Structural materials used in nuclear reactors are subject to severe conditions, such as high temperature, corrosive action of the coolant, mechanical stresses, vibration, and intense neutron irradiation. This results in rapid degradation of materials, which limits their use and may eventually cause accidents. The current objectives for nuclear-power engineering, including increasing the burn-up fraction, minimizing the amount of radioactive waste, etc., and the development of new reactor types impose even stricter requirements on the durability of structural materials. Therefore, the development of materials with improved parameters (fine mechanical strength, plasticity, radiation resistance, and corrosion resistance [1, 2]) is a crucial task.

Austenitic stainless steels and alloys are among the materials that meet the above requirements optimally. These alloys offer a well-established process technology and fine performance characteristics, are relatively cheap, and their radiation resistance is rather well-studied. However, austenitic steels and alloys are prone to radiation-induced swelling (increase in the linear dimensions under irradiation), which is the primary factor that limits their use.

The void swelling of steels and alloys is induced by the accumulation of vacancy-type defects [1–4]. This is in turn associated with the varied efficiency of absorption of vacancies and interstitial atoms, which are produced under irradiation, by sinks (dislocations, grain boundaries, etc.). The oversaturation with vacancies can be managed by introducing either a large number of additional sinks of point defects or centers that markedly enhance their recombination [5]. Coherent intermetallic Ni_3Al(Ti,Si)-type particles, which are produced in aging steels and alloys, can serve as such sinks or recombination centers. If a large number ($\sim 10^{24}$ m^{-3}) of fine precipitates coherent with the matrix are present in alloys, the swelling may be reduced by several times (compared to similar steels and alloys without precipitates) [6–8].

The effect of intermetallic precipitates on the swelling of structural materials has been discovered more than 30 years ago, but its mechanism still remains unclear. One of the primary reasons for this is the lack of systematic studies of the influence of intermetallic precipitates on the behavior of point defects under irradiation (specifically, the influence of the chemical composition of precipitate particles, their size and density, and the irradiation conditions, such as the temperature, dose, etc.). These data could shed light on the mechanisms of influence of precipitates on the accumulation of radiation defects.

It should be noted that austenitic stainless steels are multicomponent systems. They normally contain various process-related impurities (e.g., boron, carbon, and phosphorus), which may interact with defects. In addition, multiple coherent and incoherent second-phase precipitates are produced in steels in the course of thermal annealing or irradiation. They also interact with point defects. This complicates the analysis of experimental data. Therefore, the behavior of defects in model austenitic iron–nickel alloys is of considerable interest.

The study of behavior of point defects in alloys and steels at the initial stages of irradiation (up to 1 displacement per atom (dpa)) allows one to identify the specific features of interaction between radiation defects and intermetallic precipitates. Small accumulations of defects in the form of loop nucleus or three-dimensional clusters, which grow and evolve into dislocation loops or pores, respectively, form at these stages. The structure of defect accumulations that emerge at the early stages of irradiation sets the properties and the defect structure of a material irradiated to high doses (1 dpa and higher). The initial material microstructure formed prior to irradiation remains unchanged at low doses, which simplifies the analysis of the observed processes.

Positron annihilation spectroscopy (PAS) is one of the most efficient methods for examining the behavior of defects at the early irradiation stages. Positrons are a well-known probe for vacancy-type defects [9]. PAS is highly sensitive to defects in terms of their size (0.1–3 nm) and density (10^{-3}–10^{-6} per atom). Due to its high sensitivity and selectivity toward vacancy-type defects, PAS allows one to study the behavior of radiation defects at the initial stage of radiation damaging (up to 10^{-3} dpa). In addition, we have demonstrated in [10] that positrons interact with nanosized Ni_3Al precipitate particles. This results in positron confinement in intermetallic precipitates, which is induced by the preferential affinity of positrons to precipitate particles. This effect makes it possible to study the electronic and atomic structure of particles. It is hard or even impossible to obtain these data using other methods (specifically electron microscopy).

Electron irradiation is the most efficient method of defect production for studies into the interaction of defects with microstructural elements of steels and alloys. In contrast to neutron or ion irradiation, electron irradiation produces freely migrating point defects (vacancies and interstitial atoms), thus providing the opportunity to examine the interaction of defects of various types with impurities and lattice imperfections of an alloy.

We have already used PAS in [11] to study the accumulation and annealing of vacancy defects in Fe–Ni–Al alloys with different initial microstructures (solution-annealed or aged under varying conditions) at low irradiation temperatures (300–423 K). In the present study, the influence of intermetallic Ni_3Al precipitates on the accumulation of vacancy defects in the same alloy at a higher irradiation temperature of 573 K is analyzed. Some of the results presented below have already been published earlier in [12–14].

MATERIALS AND TECHNIQUES

The Fe–Ni–Al alloy containing 31.2 at % Ni and 10.8 at % Al was studied. This alloy is an aging one. Coherent particles of the γ′-phase type Ni_3Al precipitate within it in the course of annealing at temperatures above 700 K. The studied samples had the form of plates $10 \times 10 \times 0.2$ mm^3 in size. Following rolling, cutting, and electrolytic polishing, the samples were annealed at 1373 K in the atmosphere of refined helium for 1 h and subjected to water quenching at a rate of ~500 K/s. The annealing and quenching regimes were chosen so as to suppress the formation of intermetallic precipitates during cooling. The quenched samples were polished electrolytically in order to remove surface contamination. Some quenched alloy samples were annealed at 823 and 923 K for 3–35 h with subsequent water quenching.

Table 1. Fe–Ni–Al alloy aging regimes and the parameters of precipitates

Aging regime	Average particle size, nm	Particle density, 10^{22} m^{-3}	Volume fraction, %
823 K, 3 h	1	460	0.24
923 K, 3 h	5	10	0.65
923 K, 35 h	8	5.4	1.45

The microstructure and the phase composition of quenched and aged samples were examined using a JEM-200 CX transmission electron microscope (TEM) at an accelerating voltage of 160 kV and a DRON-2 X-ray diffractometer. The X-ray diffraction analysis of quenched samples revealed a 100% austenitic phase. According to the TEM data, the average grain size was ~50 μm, and the dislocation density was ~10^{11} m^{-2}.

The TEM studies of aged samples demonstrated that intermetallic particles of the Ni_3Al γ′-phase formed in the alloy after aging at 823–923 K. The size and the density of particles were determined based on dark-field images with superstructure reflections. The aging regimes and the parameters of precipitates are presented in Table 1. A detailed description of the results of an examination of the initial microstructure of aged samples was given in [13].

The alloy samples with different initial microstructures were irradiated with 5-MeV electrons from a linear accelerator at 573 K. The electron beam was scanned over the sample surface for uniform irradiation. The temperature was maintained within ~5 K of the target value in the course of irradiation. The maximum fluence was 5×10^{22} electrons/m^2. According to the results of calculations with the modified Kinchin–Pease model [15], this corresponds to a damaging dose of ~5×10^{-4} dpa.

The defect structure of samples was determined using the angular correlation of annihilation radiation (ACAR) method, which is one of the PAS techniques [9, 16]. ACAR studies were conducted using a spectrometer with a resolution of 1 mrad × 160 mrad. The

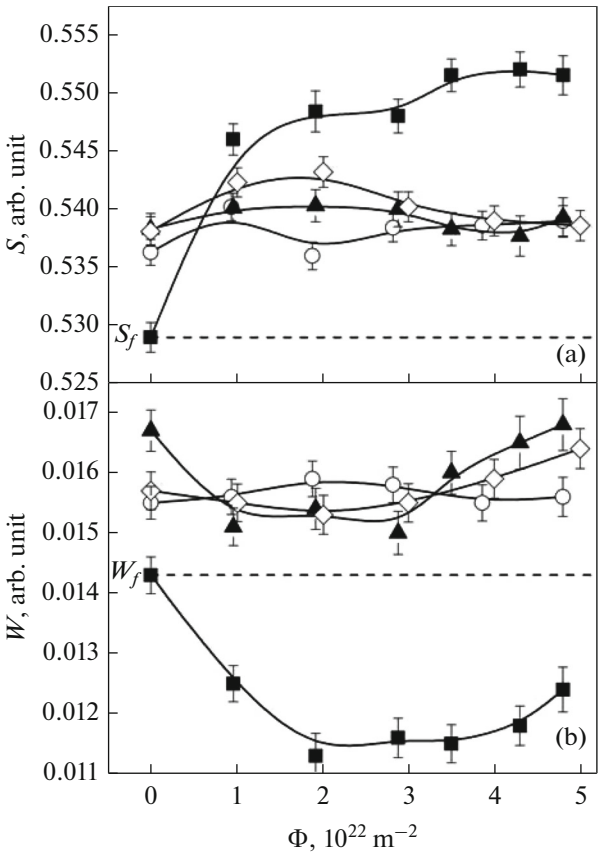

Fig. 1. Dependences of (a) S parameter and (b) W parameter on the electron fluence for different Fe–Ni–Al alloy samples irradiated at 573 K: solution-annealed sample (■) and samples containing precipitates with average sizes of 1 (○), 5 (▲), and 8 nm (◇).

^{68}Ge radionuclide with an activity of ~400 MBq served as the positron source. Approximately 5×10^5 coincidence counts were accumulated in each ACAR spectrum. All measurements were performed at room temperature. The ACAR spectra are dependences of the coincidence counting rate on angle θ (where θ is the deviation of the propagation angle of annihilation γ quanta from 180°). Angle $\theta = p_z/m_0c$, where p_z is the transverse momentum component of an electron–positron pair, m_0 is the rest mass of an electron, and c is the speed of light in vacuum. Since a positron is thermalized in the sample, θ is defined by the momentum of an annihilating electron. Thus, the ACAR spectrum characterizes the momentum distribution of annihilating electrons. The algorithm of the ACAR spectra processing was discussed in detail in [12].

The shape of the ACAR spectra changes when positrons are captured by vacancy defects or intermetallic precipitate particles, since the electron structure of defects and particles differs from that of the alloy. These changes were characterized by the standard S and W parameters defined as the ratios of areas of the low-momentum ($p_z \le 3 \times 10^{-3}\ m_0c$) and the high-momentum ($15 \times 10^{-3}\ m_0c \le p_z \le 25 \times 10^{-3}\ m_0c$) spectral regions, respectively, to the overall area under the spectrum.

The low-momentum spectral region corresponds to the annihilation of positrons with valence electrons. The variations in the ACAR spectra (and, consequently, the S parameter) in this region are governed by the density of positron trap centers. The values of the S parameter increase both with the annihilation of positrons captured by the vacancy-type defects and annihilation in the Ni_3Al particles.

The high-momentum region corresponds to the annihilation of positrons with electrons of ion cores. The electrons of inner shells are tightly bound to the nucleus and are almost unaffected by chemical bonding and the crystal structure. Therefore, the shape of the ACAR spectra in the high-momentum region (and the W-parameter value) is governed by both the density of positron trap centers and the electron-shell structure of atoms surrounding the trap center [10, 12]. A complex analysis of variations in the S and W parameters allows one to identify the density, type, and chemical environment of the positron annihilation centers.

RESULTS

Figure 1a shows the dependence of the S parameter on the electron fluence for Fe–Ni–Al samples with different initial microstructures irradiated at 573 K. Prior to irradiation, the S parameter for the solution-annealed alloy sample (series SA) matches the S_f value that characterizes the annihilation of positrons from a free (defect-free) state [11]. The initial values of the S parameter for aged alloys exceed those for the sample of the SA series.

When the solution-annealed sample is irradiated, the S parameter increases with fluence up to 2×10^{22} m^{-2} and levels off. The S parameter in aged alloys containing Ni_3Al precipitates remains almost unchanged as the fluence increases in the course of irradiation. It should be noted that positrons in aged samples can interact with both vacancies and Ni_3Al particles. Both processes result in an increase in the value of the S parameter. The dominant positron trap centers in alloy samples are discussed below.

Figure 1b presents the dependences of the W parameter on the electron fluence for alloy samples with different initial microstructures. It can be seen that the initial values (determined prior to irradiation) of the W parameter for the solution-annealed sample match the W_f value that corresponds to the annihilation of positrons from a free state. The initial values of the W parameter for alloys containing Ni_3Al precipitates exceed the W_f value, which is indicative of the positron's localization within the precipitate particles [10].

The W parameter for the solution-annealed sample decreases with an increase in fluence. This suggests that positrons are captured by vacancy-type defects. However, the W parameter increases slightly at $\Phi \geq 4 \times 10^{22}$ m^{-2}. The W parameter for the sample containing particles of Ni_3Al precipitate with an average size of 1 nm is almost independent of the fluence. In alloy samples containing Ni_3Al precipitate particles with average sizes of 5 and 8 nm, the W parameter decreases with an increase in fluence through to 3×10^{22} m^{-2}. As the fluence increases further, the W parameter for aged samples starts to increase and reaches the initial (preirradiation) value at $\Phi = 5 \times 10^{22}$ m^{-2}.

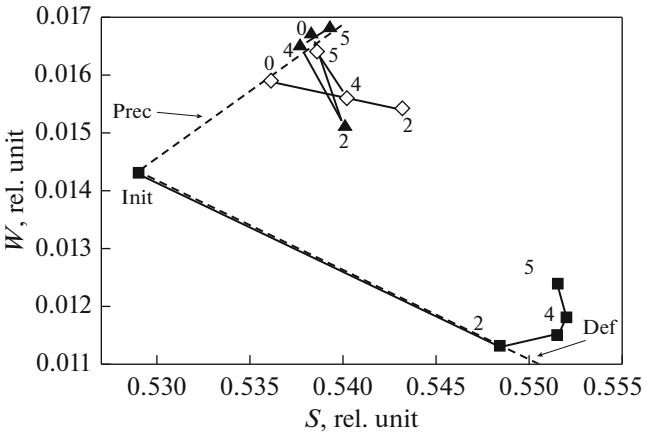

Fig. 2. S–W correlation diagram for Fe–Ni–Al alloy samples that differ in the initial microstructure and were irradiated to different fluences: solution-annealed sample (■) and the samples containing precipitates with average sizes of 1 (○), 5 (▲), and 8 (◇) nm. Numbers denote the electron fluence ($\times 10^{22}$ m^{-2}).

DISCUSSION

Dominant Positron Trap Centers in the Irradiated Fe–Ni–Al Alloy

The S–W plot in Fig. 2 is a convenient tool for identifying the type of positron trap centers dominant in alloys with different initial microstructures. The "Init" point in Fig. 2 is the initial point that corresponds to the annihilation of positrons from a free state, i.e., to the annihilation parameters for the solution-annealed alloy in the nonirradiated state. The numbers in Fig. 2 denote the electron fluence ($\times 10^{22}$ m^{-2}). If only one type of trap center is present in an alloy, the corresponding points lie on a single straight line passing through the initial point. The slope of this line characterizes the type of positron trap centers, and the distance between the point of interest and the initial point corresponds to the density of trap centers of the respective type. The lines that correspond to the annihilation of positrons captured by vacancy defects and intermetallic precipitate particles are denoted as "Def" and "Prec" in Fig. 2, respectively.

It can be seen that the points for the solution-annealed alloy irradiated with electrons to $\Phi = 2 \times 10^{22}$ m^{-2} lie on the "Def" line. This suggests that, here, positrons are captured only by vacancy-type defects. As the fluence increases further, the points shift upward. This is indicative of the emergence of other positron trap centers. We have demonstrated recently in [17] that the radiation-induced formation and growth of intermetallic nanoparticles occur in the Fe–Ni–Al alloy in the course of irradiation at 573 K. It was already noted that these particles are positron trap centers. Thus, the upward shift of points away from the "Def" line provides evidence of the positron capture both by vacancy-type defects and nanosized Ni_3Al particles.

The position of points for the aged alloy that contains precipitate particles with an average size of 1 nm remains almost unchanged as the fluence increases. This suggests that positrons annihilate exclusively from the Ni_3Al-captured state, and the size and the density of Ni_3Al nanoparticles do not change upon irradiation. This also demonstrates that vacancies are lacking in the irradiated alloy. Thus, ultrafine precipitate particles completely suppress the accumulation of vacancies in the course of irradiation at the given temperature.

When the fluence increases, the points for the alloy containing precipitate particles with an average size of 5 nm shift downward. This is attributed to the partial capture of positrons by vacancy defects. At the same time, positrons are also captured here by precipitate particles. The curve rises again as the fluence increases further, and the annihilation parameters for the irradiated alloy at $\Phi \geq 4 \times 10^{22}$ m^{-2} are almost the same as those corresponding to the initial (nonirradiated) alloy. This implies that the fraction of positrons captured by vacancy defects decreases at higher fluences, while the fraction of positrons localized within precipitates increases. It also follows that the vacancies formed at low fluences are annealed completely at sinks or recombine with interstitial atoms in the course of further irradiation. Just as in the solution-annealed alloy, secondary precipitate particles emerge here after irradiation [17]. As a result, the overall density of precipitates present in the alloy increases, which enhances the influence of precipitates on the behavior of defects under irradiation.

A similar effect is also observed in the sample containing Ni_3Al precipitate particles with an average size of 8 nm (see Fig. 2). It should be noted that the point that corresponds to a fluence of 5×10^{22} m^{-2} in this alloy lies further away from the Init point than the initial (preirradiation) point. Therefore, the density of precipitates or their size increase in this alloy under irradiation.

Possible Mechanisms of Interaction between Coherent Precipitate Particles and Point Defects

The data presented above demonstrate that precipitate particles affect the accumulation of vacancy defects in the course of irradiation at 573 K. It should be noted that the capture of positrons by vacancy defects is transition-limited: the annihilation characteristics are governed by the probability of the positron transition from a free state to a localized one [18]. Capture by precipitates is diffusion-limited, and the annihilation characteristics are governed here by the ratio between the diffusion length of a positron and the average distance between precipitates [19]. Since mathematical models for calculating the defect density from annihilation parameters of alloys with both types of positron trap centers present are lacking in the literature, we did not determine the density of vacancies produced in alloys after irradiation at 573 K. However, it follows from the results of qualitative analysis (see above) that the rate of the accumulation of vacancy defects under irradiation in aged alloys is lower than the corresponding rate in solution-annealed alloys. The accumulation of vacancy defects is not observed at all in alloy containing precipitates with average sizes of 1 nm.

We have demonstrated in [11] that precipitates enhance the mutual recombination of defects. This effect is attributed to the influence of elastic-stress fields, which emerge at the precipitate–matrix boundary due to the difference in lattice parameters between the precipitate and the matrix. Since the lattice parameter of Ni_3Al is lower than that of the alloy matrix, compression stresses emerge at the precipitate–matrix boundary. According to the hypothesis put forth by the authors of [20], interstitial atoms (IAs) produced upon irradiation move away from precipitates under the influence of elastic stresses, while vacancies move in the opposite direction. Thus, point defects move toward each other, which enhances their mutual recombination.

Precipitates can also serve as sinks for point defects. Due to the presence of elastic stresses at the precipitate–matrix boundary, precipitates capture migrating point defects. The capture of defects of opposite types leads to their mutual recombination at the precipitate–matrix boundaries. This also enhances the mutual recombination of point defects.

It should be noted that precipitates can serve as weak sinks for point defects [21], since the magnitude of elastic stresses that act at the precipitate–matrix boundary and, consequently, the precipitate–defect binding energy are rather low [22]. The defects captured by the precipitate–matrix boundaries are then emitted back into the alloy matrix with a certain delay, which results in the additional enhancement of the mutual recombination of point defects [21, 23–25]. Since IAs have a higher mobility than vacancies, they reach the boundaries of precipitates first and are captured by them. These IAs are emitted back into the alloy matrix with a certain delay, which is defined by the IA–precipitate binding energy, and recombine with vacancies. As a result, regions of enhanced recombination of point defects form around precipitates [25, 26]. The radius of these regions depends on the mobility of point defects and, consequently, increases with temperature. The overall volume of these regions is directly proportional to the density of precipitates. Thus, the efficiency of precipitates increases with the irradiation temperature and the degree of dispersion of precipitates, which is what was observed in the experiment.

Another feature of the studied alloy should be noted. We have demonstrated in [11] that the effect observed under irradiation at 423 K was strongest in the alloy containing precipitates with an average size of 5 nm. The rate of accumulation of vacancy defects under irradiation in the alloy containing particles with an average size of 1 nm was only slightly lower than the rate of defect accumulation in the annealed alloy. However, in the case of irradiation at 573 K, the effect was strongest in the alloy with 1-nm particles. We have hypothesized in [11] that the majority of particles here are seed precipitates, which have almost no effect on the behavior of point defects. It is fair to assume that, due to radiation-induced aging, these seeds transformed into the proper γ'-phase at the very beginning of irradiation at 573 K. As a result, the density and the efficiency of Ni_3Al precipitates in the alloy increased. The precipitate structure remained unchanged at later stages, which is attributed to the short distance between the precipitates and, consequently, to the short free path of defects. The effect may also be caused by the operation of several mechanisms of the precipitate–point defect interactions with their efficiencies, which depend in various ways on the irradiation conditions and the initial microstructure of the alloy.

CONCLUSIONS

The influence of intermetallic Ni_3Al precipitates on the accumulation of vacancy defects in the aged Fe–Ni–Al alloy under irradiation at a temperature of 573 K was studied using positron annihilation spectroscopy. It was found that intermetallic precipitate particles inhibit the process of the accumulation of vacancy defects at the initial stages of irradiation (10^{-4} dpa). This effect depends on the size, density, and type of particles. The results of analyzing the experimental data suggest that precipitates facilitate the mutual recombination of point defects that form under irradiation. This is attributed to elastic stresses at the precipitate–matrix boundaries.

ACKNOWLEDGMENTS

This study was conducted under state assignment from the Federal Agency for Scientific Organizations (project Spin, no. AAAA-A18-118020290104-2) with partial support from the Russian Foundation for Basic Research (project no. 18-02-00270).

REFERENCES

1. S. J. Zinkle and J. T. Busby, "Structural materials for fission & fusion energy," Mater. Today. **12**, 12–19 (2009).
2. S. J. Zinkle and G. S. Was, "Materials challenges in nuclear energy," Acta Mater. **61**, 735–758 (2013).
3. V. F. Zelenskii, I. M. Neklyudov, and T. P. Chernyaeva, *Radiation defects and swelling of metals* (Naukova dumka, Kiev, 1988) [in Russian].
4. J. F. Bates and R. W. Powell, "Irradiation-induced swelling in commercial alloys," J. Nucl. Mater. **102**, 200–213 (1981).
5. R. Bullough, B. L. Eyre, and G. L. Kulcinski, "A systematic approach to the radiation damage problem," J. Nucl. Mater. **68**, 168–178 (1977).
6. V. V. Sagaradze and S. S. Lapin, "Unconventional approaches to the suppression of irradiation-induced swelling of stainless steels," Phys. Met. Metallogr. **83**, 417 (1997).
7. V. V. Sagaradze, B. N. Goshchitskii, V. L. Arbuzov, and Yu. N. Zuev, "Precipitation-hardening austenite steel for fast neutron reactors," Metalloved. Term. Obrab. Met. No. **8**, 13–20 (2003).
8. G. R. Odette, M. J. Alinger, and B. D. Wirth, "Recent developments in irradiation resistant steels," Annu. Rev. Mater. Res. **38**, 471–503 (2008).
9. V. I. Grafutin and E. P. Prokop'ev, "Positron annihilation spectroscopyin materials structure studies," Phys.–Usp. **45**, 59–74 (2002).
10. A. P. Druzhkov, D. A. Perminov, V. L. Arbuzov, N. N. Stepanova, N. L. Pechorkina, "Positron confinement in intermetallic nanoparticles embedded in Fe–Ni–Al material," J. Phys.: Condens. Matter. **16**, 6395–6404 (2004).
11. D. A. Perminov, A. P. Druzhkov, and V. L. Arbuzov, "Positron-annihilation studies of the influence of nanodimensional intermetallic precipitates on the evolution of radiation defects in the Fe–Ni–Al alloy," Phys. Met. Metallogr. **116**, 1151–1158 (2015).
12. A. P. Druzhkov, D. A. Perminov, and V. L. Arbuzov, "Effects of intermetallic nanoparticles on the evolution of vacancy defects in electron irradiated Fe–Ni–Al material," J. Phys.: Condens. Matter. **18**, 365–377 (2006).
13. A. P. Druzhkov, D. A. Perminov, and N. L. Pecherkina, "Positron annihilation spectroscopy characterization of effect of intermetallic nanoparticles on accumulation and annealing of vacancy defects in electron-irradiated Fe–Ni–Al alloy," Philos. Mag. **88**, 959–976 (2008).
14. D. A. Perminov, A. P. Druzhkov, and V. L. Arbuzov, "Role of intermetallic nanoparticles in radiation damage of austenitic Fe–Ni-based alloys studied by positron annihilation," J. Nucl. Mater. **414**, 186–193 (2011).
15. J. Morillo, C. H. de Novion, and J. Dural, "Neutron and electron radiation defects in titanium and tantalum monocarbides: An electrical resistivity study," Radiat. Eff. **55**, 67–78 (1981).
16. M. Eldrup and B. N. Singh, "Studies of defects and defect agglomerates by positron annihilation spectroscopy," J. Nucl. Mater. **251**, 132–138 (1997).
17. A. P. Druzhkov, S. E. Danilov, D. A. Perminov, and V. L. Arbuzov, "Formation and evolution of intermetallic nanoparticles and vacancy defects under irradiation in Fe–Ni–Al ageing alloy characterized by resistivity measurements and positron annihilation," J. Nucl. Mater. **476**, 168–178 (2016).
18. L. C. Smedckjaer and M. J. Fluss, "Experimental methods of positron annihilation for the study of defects in metals," Methods Exp. Phys. **21**, 77–145 (1983).
19. M. A. van Huis, A. van Veen, H. Schut, C. V. Falub, S. V. H. Eijt, P. E. Mijnarends, and J. Kuriplach, "Positron confinement in embedded lithium nanoclusters," Phys. Rev. B. **65**, 085416 (2002).
20. A. N. Orlov, A. M. Parshin, and Yu. V. Trushin, "Physical aspects of weakening of radiation swelling of construction alloys," Zh. Tekh. Fiz. **53**, 2367–2372 (1983).
21. B. P. Uberuaga, S. Choudhury, and A. Caro, "Ideal sinks are not always ideal: Radiation damage accumulation in nanocomposites," J. Nucl. Mater. **462**, 402–408 (2015).
22. A. J. Ardell, B. Mastel, and J. J. Laidler, "High-voltage electron irradiation studies of several overaged γ/γ' alloys," J. Nucl. Mater. **54**, 313–324 (1974).
23. I. J. Beyerlein, M. J. Demkowicz, A. Misra, and B. P. Uberuaga, "Defect-interface interactions," Prog. Mater. Sci. **74**, 125–210 (2015).
24. Z. Bi, B. P. Uberuaga, L. J. Vernon, J. A. Aguiar, E. Fu, S. Zheng, S. Zhang, Y. Wang, A. Misra, and Q. Jia, "Role of the interface on radiation damage in the $SrTiO_3/LaAlO_3$ heterostructure under Ne^{2+} ion irradiation," J. Appl. Phys. **115**, 124315 (2014).
25. X.-Y. Liu, B. P. Uberuaga, M. J. Demkowicz, T. C. Germann, A. Misra, and M. Nastasi, "Mechanism for recombination of radiation-induced point defects at interphase boundaries," Phys. Rev. B **85**, 012103 (2012).
26. M. J. Demkowicz, R. G. Hoagland, B. P. Uberuaga, and A. Misra, "Influence of interface sink strength on the reduction of radiation-induced defect concentrations and fluxes in materials with large interface area per unit volume," Phys. Rev. B **84**, 104102 (2011).

Translated by D. Safin